XIV International Conference on Topics in Astroparticle and Underground Physics (TAUP 2015) IOP Publishing
Journal of Physics: Conference Series **718** (2016) 052037 doi:10.1088/1742-6596/718/5/052037

Measurement of the mass composition of ultra-high energy cosmic rays with the Pierre Auger Observatory

Mariangela Settimo[1], for the Pierre Auger Collaboration[2]

[1] Laboratoire de Physique Nucléaire et de Hautes Energies (LPNHE), CNRS-IN2P3, Paris, France
[2] Observatorio Pierre Auger, Av. San Martín Norte 304, 5613 Malargüe, Argentina

E-mail: mariangela.settimo@lpnhe.in2p3.fr
Full author list: *http://www.auger.org/archive/authors_2015_09.html*

Abstract. The understanding of the nature of ultra-high energy cosmic rays is one of the most intriguing open questions for current and future observatories. With its hybrid design and huge exposure, the Pierre Auger Observatory provides valuable statistical measurements of the chemical composition of cosmic rays with energies above 10^{17} eV, including the search for neutral primaries such as neutrinos and photons. We report on the most recent results which are based on the accurate measurement of the depth of the shower maximum, $X_{\rm max}$, by the fluorescence telescopes and on the shape of the signals recorded by the water-Cherenkov detectors. The interpretation of these results in terms of mass composition is also discussed related to the hadronic interaction models used to describe the development of air showers.

1. Introduction

The chemical composition of ultra-high energy cosmic rays (UHECRs) is still uncertain as its determination strongly relies on the knowledge of the air-shower development and on the extrapolation of the hadronic interactions in an energy regime not accessible with the accelerators. A measurement of the mass composition has been performed by the Pierre Auger Collaboration at energies above 10^{17} eV. The Pierre Auger Observatory [1] is located in Argentina, in the province of Mendoza. It consists of an array of 1660 water Cherenkov stations (surface detector, SD) deployed over an area of 3000 km^2. The array is overlooked by a fluorescence detector (FD) consisting of of 27 telescopes which operate during clear and moonless nights (with a total duty cycle of about 13%). Among them, 24 regular telescopes have a field of view between 1° and 30° in elevation and three High Elevation Auger Telescopes (HEAT) have been recently added and are stably taking data since 2012. The new telescopes have the advantage of operating in downward mode (field of view of between 0° and 30° in elevation angle) and upward mode (field of view between 30° and 60°). They are located close to one of the FD sites, Coiuheco, allow a combined observation of the longitudinal profiles over a wide elevation angle and enable additional cross-calibrations. Hybrid events are formed when at least one fluorescence telescope and one SD station are triggered in coincidence. The FD observes the longitudinal development of the air-shower in atmosphere allowing the direct determination of the depth ($X_{\rm max}$) at which the shower reaches its maximum and that is a well known mass

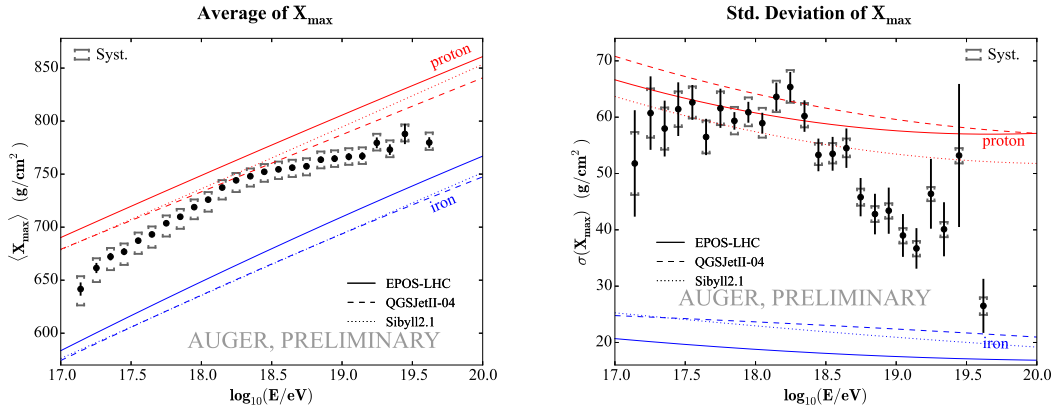

Figure 1. Evolution of the first two moments of the $X_{\rm max}$ distribution with energy. Expectation for proton and iron primaries are shown as lines for different hadronic interaction models.

composition sensitive parameter. In addition, the SD samples the density of secondary particles at the ground and can thus be used to indirectly derive the muonic content, which is also related to the mass of the primary cosmic ray.

2. Observation of the longitudinal profile

The longitudinal profile is reconstructed by means of the fluorescence (and Cherenkov) light detected by the FD. The determination of the primary composition is based on the measurement of the first two moments of the $X_{\rm max}$ distribution ($\langle X_{\rm max}\rangle$ and $\sigma(X_{\rm max})$) which are related to the $\ln A$ and $\sigma(\ln A)$, with A the atomic mass of the primary cosmic ray. The analysis is performed using hybrid data selected with strict criteria to ensure high quality longitudinal profiles and to avoid any possible bias introduced by the limited field of view of the FD. 18382 events with energy above $10^{17.8}$ eV are selected among the data collected by the regular FD between December 2004 and December 2012. 5490 events (with energy between 10^{17} eV and $10^{18.3}$ eV) are added using the dataset of events observed at the same time by the HEAT and the Coihueco sites between June 2010 and August 2012. A detailed discussion of these two datasets and the comparison between them is given in [2]. The $X_{\rm max}$ is determined with a resolution of about 25 g/cm^2 at very low energy decreasing down to about 15 g/cm^2 above 10^{18} eV [3, 2]. The systematic uncertainties are estimated to be smaller than 10 g/cm^2 and they include the reconstruction, calibration and atmospheric contributions.

The evolutions of $\langle X_{\rm max}\rangle$ and $\sigma(X_{\rm max})$ with energy are shown in Figure 1, left and right, respectively, for the combined dataset. Between $10^{17.0}$ and $10^{18.3}$ eV $\langle X_{\rm max}\rangle$ increases by around 85 g cm^{-2} per decade of energy. This value is larger than the one expected for a constant mass composition indicating that the mean primary mass is getting lighter. Around $10^{18.3}$ eV a break is observed suggesting a change of composition towards heavier nuclei. These conclusions are also confirmed by the trend of $\sigma(X_{\rm max})$. The average $X_{\rm max}$ and the $\sigma(X_{\rm max})$ can be converted to mass by means of simulations. The corresponding plots are shown in Figure 2, where $\ln A$ (top) and its variance $\sigma^2(\ln A)$ (bottom) are given for three hadronic models (from left to right). The shaded band delimits to a region of unphysical values. In the $\ln A$ plot, a value equal to zero corresponds to a pure proton composition and the maximum value of four to a pure iron assumption. The values of $\sigma^2(\ln A)$ can range between zero and four representing a pure composition and a 50% proton 50% iron mixture, respectively. The general trend of changing composition discussed so far is observed in all the hadronic models. Furthermore, the variance of $\ln A$ is almost constant below $10^{18.3}$ eV and then decreases, indicating that composition changes

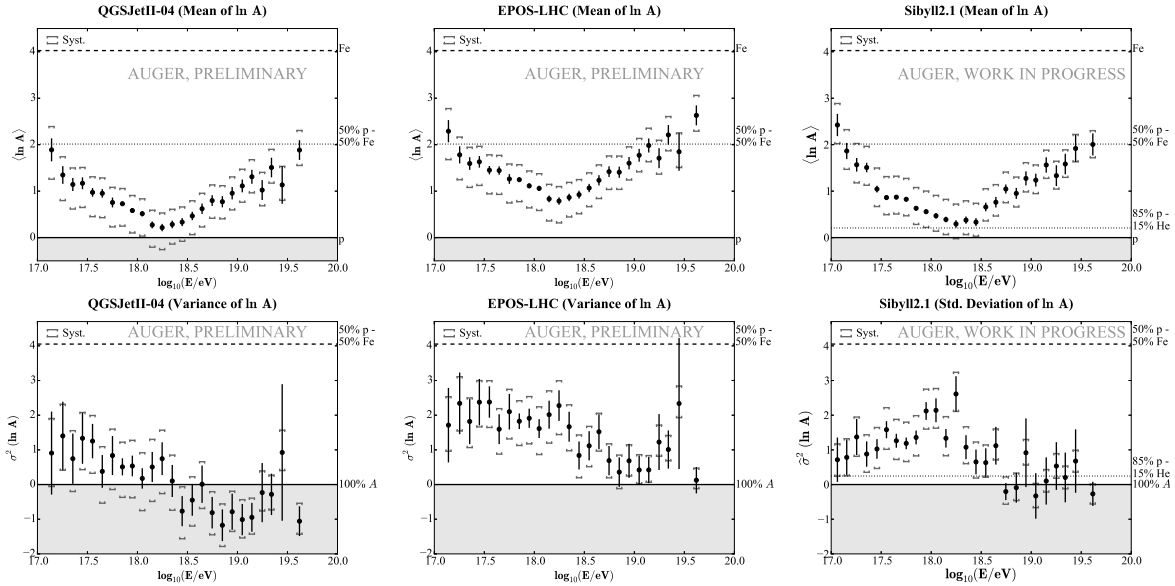

Figure 2. The average of the logarithmic mass (top) and its variance (bottom) estimated from data for three hadronic interaction models [6, 7, 8]. The shaded area denote the non-physical region.

from a mixture of several components to one dominated by a few elements. Despite that, it has to be noted that the data at high energy seems to disfavor the QGSJET-II.04 [6] model as their interpretation using this model enters the region of unphysical results.

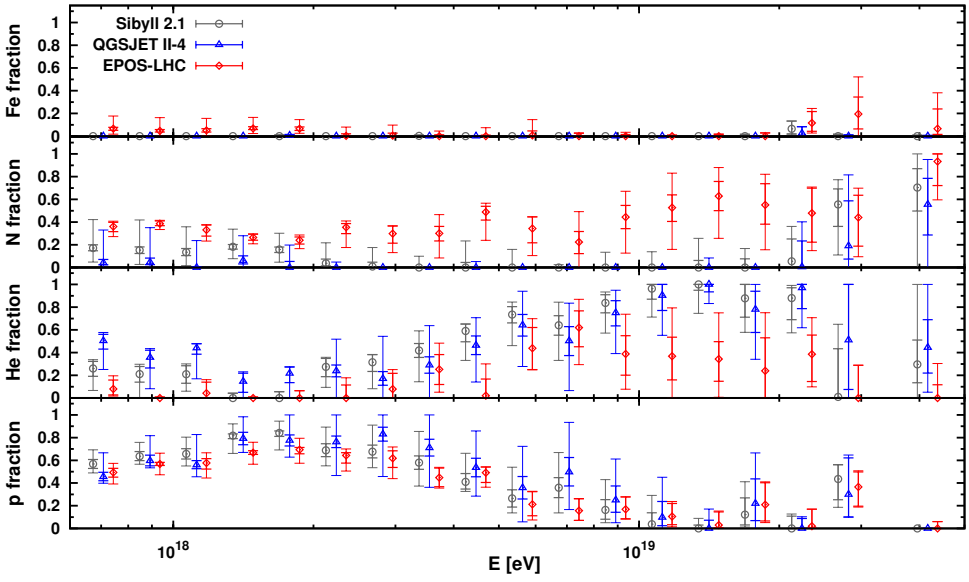

Figure 3. Fitted fraction of a mixture of four species: proton, helium, nitrogen, iron (from bottom to top) and for different hadronic models.

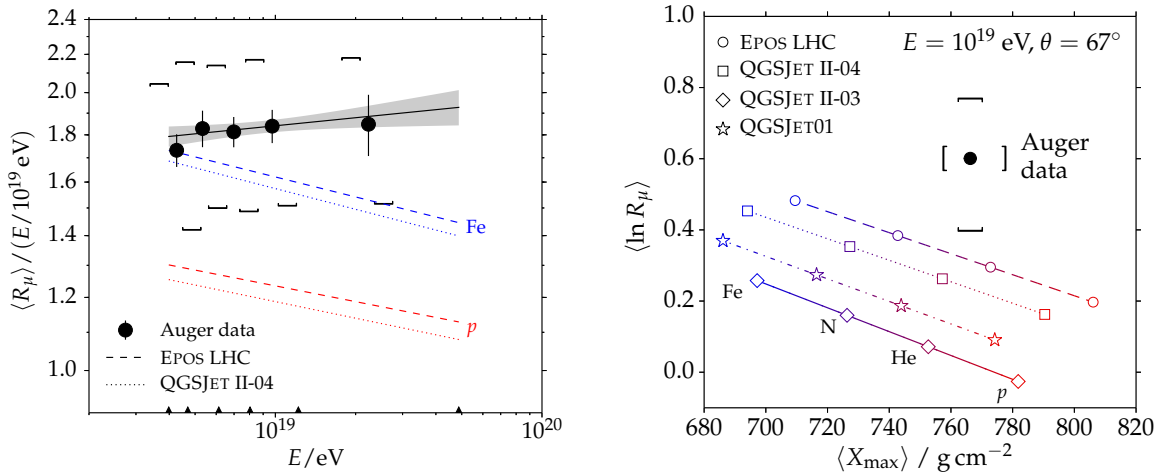

Figure 4. Left: $\langle R_\mu \rangle$ as a function of energy from data and simulations. Right: $\langle \ln R_\mu \rangle$ vs $\langle X_{\mathrm{max}} \rangle$ as derived from data and simulations at 10^{19} eV and zenith of 67°. Systematic uncertainties indicated by brackets.

2.1. Implications for mass composition

It has been shown [4] that the same values of the moments of the X_{max} distribution described above can be obtained from distributions produced with different mass composition mixtures. To avoid this degeneracy and to extract the maximum of information the full X_{max} distribution is fitted with templates obtained with simulations. A binned maximum-likelihood method is used to search for the best combination of species which matches the data. The best description of data is obtained with four components (proton, helium, nitrogen and iron nuclei) while the addition of more species does not improve the quality of the fit. The abundances of the four primary species are shown in Figure 3 as a function of energy and for three different hadronic models. All the models predict similar fractions of protons with a significant change over the energy range. On the contrary, different features are observed for the intermediate masses with QGSJET-II.04, favoring helium, and Epos-LHC suggesting a mixed composition dominated by Nitrogen.

3. Measurement of the muon content in highly inclined events

Thanks to the hybrid design of the Pierre Auger Observatory the measurement of the X_{max} can be complemented with the indirect determination of the muon content in the air shower which is a quantity proportional to the mass composition and only slightly dependent on energy. As the current surface detector does not allow for a separate measurement of muonic and electromagnetic components, the analysis is performed using inclined events for which the larger depth of traversed atmosphere acts as a shield of the electromagnetic component.

Hybrid events with zenith angle between 62° and 80° and energy above 4×10^{18} eV are selected between January 2004 and January 2013. The number of muons is determined using the relative scale factor N_{19} which relates the observed muon densities at the ground to the average muon density profile $\rho_{\mu,19}$ of proton showers at 10^{19} eV simulated with QGSJET-II.03 model [9]. The dependence on zenith angle is included in the parameterization. More details about the robustness of N_{19} against hadronic models and zenith angle are provided in [5].

A parameter, R_μ has been introduced for this analysis: It is defined as the ratio of the measured number of muons and the expected value of N_{19} obtained integrating the reference

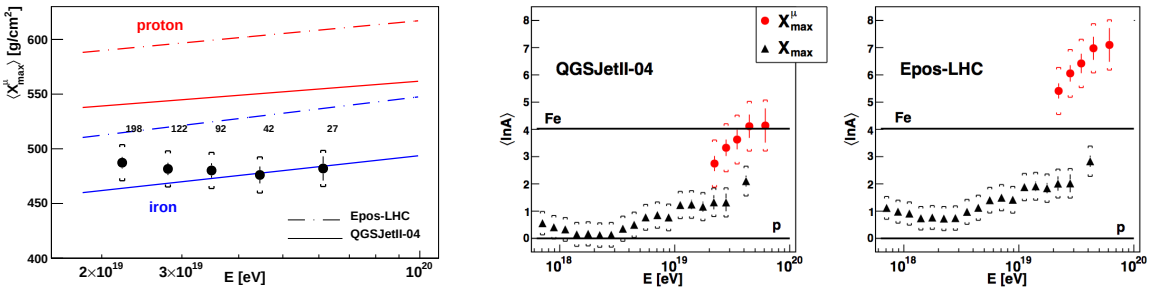

Figure 5. Left: Evolution of $X^{\mu}_{\rm max}$ with energy for data and simulations. Systematic uncertainties are indicated by brackets. Middle and right panels: $X^{\mu}_{\rm max}$ data converted to average ln$A$ are compared to results derived from the FD measurement of $X_{\rm max}$ for two hadronic models.

model $\rho_{\mu,19}$. In Figure 4, R_{μ} is shown as a function of energy (left) compared to the predictions for proton and iron simulations assuming QGSJET-II.04 and EPOS-LHC models. The separation between the expectations for proton and iron induced showers proves the power of R_{μ} as a composition estimator. The measured muon number, higher than for the pure iron case, is not compatible with simulations. The $X_{\rm max}$ and logarithm of R_{μ} measured in data are compared to values from simulations at 10^{19} eV with different models and primary species. The discrepancy between data and models confirms a muon deficit in simulations, varying between 30 and 80% depending on the hadronic model. The systematic uncertainties on R_{μ} (shown in figure as brackets) are mostly due to the energy scale and, although they limit the sensitivity of R_{μ} to mass composition, they are valuable for testing the hadronic interaction models, especially once combined with independent measurements.

4. Muon Production Depth

The time structure of the muon component reaching the ground can be exploited to obtain the distribution of distances of the muon production points along the shower axis [10, 11]. By deriving the muon production depth (MPD) [13], the longitudinal profile of the muonic component and the depth of its maximum, $X^{\mu}_{\rm max}$, are reconstructed in SD data collected between January 2004 and December 2012, with energy above $2{\times}10^{19}$ eV and zenith angle between 55° and 65°. Only stations at distances larger than 1700 m from the shower axis are used to estimate the MPD. These criteria are motivated by the necessity to reduce the electromagnetic contamination in the recorded traces and possible artificial distorsions of the MPD while the energy threshold ensures that enough muons are detected in the station. After applying additional selection cuts for a good reconstruction of the events [12], a resolution of about 100 (80) g/cm^2 is found for proton (iron) improving to 50 g/cm^2 with increasing energy. The systematic uncertainties are estimated to be around 17 g/cm^2 and are mostly due to the reconstruction, the hadronic interaction models and the seasonal effects. The evolution of $X^{\mu}_{\rm max}$ with energy is shown in Figure 5 (left) together with predictions for proton and iron simulations assuming two hadronic models. Data are well bracketed between proton and iron for the QGSJET-II.04 model, indicating a heavy composition, while they do not match the Epos-LHC model. The measured $X^{\mu}_{\rm max}$ has been converted to ln$A$ and is shown in Figure 5 (middle and right) compared to the $X_{\rm max}$ measured by FD. Results obtained for the QGSJET-II.04 model are compatible with the expected values even though this model was disfavored by the FD measurement of $X_{\rm max}$. On the contrary for the EPOS-LHC model the value of $X^{\mu}_{\rm max}$ is significantly larger than the expectation for iron and in disagreement with the $X_{\rm max}$ measurements.

5. Summary

The mass composition measured using both the surface and fluorescence detectors has been reported. The average composition has been derived from the first two moments of the $X_{\rm max}$ distribution over a wide energy range, between 10^{17} eV and a few times 10^{19} eV. Moreover, the full $X_{\rm max}$ distribution has been fitted with simulated templates to derive the fraction of each species in a mixture of N-elements, finding the best description of data for N equal to 4. Current results suggest a quite complex scenario with a composition changing with energy from a mixed to light at energy below $10^{18.3}$ eV and then increasing towards heavier primaries and dominated by a few components. Complementary to FD, two analyses have been presented based on the SD estimate of the muon content and its longitudinal development in inclined events. Both measurements show a deficit of muons in simulations whose entity depends on the assumed hadronic model. This result is compatible with the study performed with hybrid events at zenith angle smaller than 60° [14]. The current systematic uncertainties for the SD muon analyses and the disagreement with simulations do not allow us to derive conclusions on the mass. However interesting insights on hadronic models can be obtained especially in combination with the FD observation of $X_{\rm max}$. Addressing these questions is one of the goal of the proposed upgrade of the Auger Observatory described in [15, 16].

5.1. Acknowledgments

The work of M.S., made in the ILP LABEX (under reference ANR-10-LABX-63), is supported by French state funds managed by the ANR within the Investissements d'Avenir programme under reference ANR-11-IDEX-0004-02.

References

[1] Aab A *et al* (Pierre Auger Collaboration) 2015 *NIM A* **798** 172
[2] Porcelli A for the Pierre Auger Collaboration 2015 *Proc. 34th ICRC* The Hague, The Netherlands *Preprint* arXiv:1509.03732
[3] Aab A *et al* (Pierre Auger Collaboration) 2014 *Phys. Rev. D* **90** 122005
[4] Aab A *et al* (Pierre Auger Collaboration) 2014 *Phys. Rev. D* **90** 122006
[5] Aab A *et al* (Pierre Auger Collaboration) 2015 *Phys. Rev. D* **91** 032003; Errata 2015 *Phys. Rev. D* **91** 059901
[6] Ostapchenko S 2011 *Phys. Rev. D* **83** 014018
[7] Werner K, Karpenko I and Pierog T 2011 *Phys. Rev. Lett.* **106** 122004
[8] Ahn E, Engel R, Gaisser T, Lipari P, Stanev T 2009 *Phys. Rev. D* **80** 094003
[9] Ostapchenko S 2006 *Phys. Rev. D* **74** 014026
[10] Cazon L, Vazquez R, Watson A and Zas E 2004 *Astropart. Phys.* **21** 71
[11] Cazon L, Conceicao R, Pimenta M and Santos E 2012 *Astropart. Phys.* **36** 211
[12] Collica L for the Pierre Auger Collaboration 2015 *Proc. 34th ICRC* The Hague, The Netherlands *Preprint* arXiv:1509.03732
[13] Aab A *et al.* (Pierre Auger Collaboration) 2014 *Phys. Rev. D* **90** 012012; Errata 2014 *Phys. Rev. D 90* 039904(E) (2014); Errata 2015 *Phys. Rev. D* **92** 019903
[14] Farrar G for the Pierre Auger Collaboration 2013 *Proc. 33rd ICRC* Rio de Janeiro, Brazil *Preprint* arXiv:1307.5059
[15] Engel R for the Pierre Auger Collaboration 2015 *Proc. 34th ICRC* The Hague, The Netherlands *Preprint* arXiv:1509.03732
[16] Bertou X for the Pierre Auger Collaboration this conference